Energy & Environmental Science

REVIEW

View Article Online
View Journal | View Issue

Cite this: *Energy Environ. Sci.*, 2017, **10**, 846

Three dimensional printing of components and functional devices for energy and environmental applications

J. C. Ruiz-Morales,*[a] A. Tarancón,*[b] J. Canales-Vázquez,[c] J. Méndez-Ramos,[d] L. Hernández-Afonso,[a] P. Acosta-Mora,[d] J. R. Marín Rueda[c] and R. Fernández-González[a]

Received 3rd December 2016,
Accepted 28th February 2017

DOI: 10.1039/c6ee03526d

rsc.li/ees

Three dimensional printing technologies represent a revolution in the manufacturing sector because of their unique capabilities for increasing shape complexity while reducing waste material, capital cost and design for manufacturing. However, the application of 3D printing technologies for the fabrication of functional components or devices is still an almost unexplored field due to their elevated complexity from the materials and functional points of view. This paper focuses on reviewing previous studies devoted to developing 3D printing technologies for the fabrication of functional parts and devices for energy and environmental applications. The use of 3D printing technologies in these sectors is of special interest since the related devices usually involve expensive advanced materials such as ceramics or composites, which present strong limitations in shape and functionality when processed with classical manufacturing methods. Recent advances regarding the implementation of 3D printing for energy and environmental applications will bring competitive advantages in terms of performance, product flexibility and cost, which will drive a revolution in this sector.

Broader context

Intensive research on additive manufacturing has been carried out during the last three decades to allow the fabrication of three dimensional objects by assembling materials without the use of tools or molds. Three dimensional printing technologies represent a potentially low-cost, new paradigm for the manufacture of energy conversion technologies offering unique capabilities in terms of shape/geometry complexity and enhancement of specific performance per unit of mass and volume of the 3D printed units. However, the fabrication of highly complex devices for the energy sector by using 3D printing is an almost unexplored field. In this work we review the state of the art of 3D printing technology to fabricate components or devices for energy and environmental applications, focusing on aspects related to the control of the microstructure, functionality and performance of the 3D printed structures.

1. Introduction

Additive manufacturing (AM) is the process of making a three dimensional solid object by adding layer-upon-layer of material starting from a digital computer model designed using modeling software, often called CAD (Computer-Aided Design). AM, popularly called 3D printing,[1] is achieved using an additive process, where successive layers of material are laid down in different shapes. This makes it quite different from traditional machining techniques, which mostly rely on the removal of materials by methods such as cutting or drilling (subtractive processes). Objects that are manufactured additively can be used anywhere throughout the product life cycle, from pre-production (*i.e.*, rapid prototyping) to full-scale production (*i.e.*, rapid manufacturing), in addition to tooling applications and post-production customization. Today this technology is already extensively used in the jewelry, footwear, industrial design, architecture, engineering, automotive, aerospace, dental and medical industries[2] but, more interestingly, a market between $230 billion and $550 billion is expected by 2025.[3]

The renewable energy sector is one of the fastest growing sectors in the world due to the devastating effects of global warming, mainly caused by the massive use of fossil fuels.

[a] *Dpto de Química, U.D. Química Inorgánica, Universidad de La Laguna, 38206 La Laguna, Tenerife, Spain. E-mail: jcruiz@ull.edu.es*
[b] *IREC, Catalonia Institute for Energy Research, Advanced Materials for Energy, 08930, Sant Adrià del Besòs, Barcelona, Spain. E-mail: atarancon@irec.cat*
[c] *Instituto de Energías Renovables, PRINT3D SOLUTIONS, Universidad de Castilla la Mancha, 02006, Albacete, Spain*
[d] *Departamento de Física, Universidad de La Laguna, 38206 La Laguna, Tenerife, Spain*

The development of some of these sustainable technologies is closely related to the implementation of a hydrogen economy. Hydrogen can be produced from renewable energies by photocatalytic water splitting[4] or through thermolysis using concentrating solar power[5] and stored in several types of materials, or even in the current natural gas network, to be used afterwards for providing power through Solid Oxide Fuel Cells (SOFCs).[6] Most of the components used in the aforementioned applications are based on ceramics, composites or cermets with exceptional properties that strongly depend on special compositions and microstructures. The design of these microstructures can critically affect key parameters such as performance, mechanical stability, optimisation of gas flow-paths to/from the reaction sites, thermal instability and, depending on the materials, resiliency to redox cycling. Furthermore, in most of the cases, any engineered microstructure must be stable at high temperatures, *e.g.* metal oxides (Zn and Fe)[7] reach temperatures in excess of 1500 °C in typical thermo-cycles of concentrating solar power and Yttria-Stabilized Zirconia (YSZ)-based components need to be sintered at 1400 °C to produce gas-tight materials for SOFC applications. In this sense, the unique capabilities of 3D printing for implementing hierarchical, material and functional complexity can be an ideal approach to precisely engineer ceramics/composites/cermet microstructures required for these highly demanding applications.[2,8,9] Moreover, using 3D printing technologies significantly reduces the production costs by preventing the loss of valuable advanced materials while simplifying the design for manufacturing and reducing the number of fabrication steps (shaping, thermal treatments and assembly).

Although intensive research on additive manufacturing has been carried out during the last three decades,[10,11] shaping process technologies for functional materials, in particular ceramics and composites, are still important challenges due to the fact that additive manufacturing techniques have been mainly developed and commercialized for polymeric and metallic structural parts.[9,12] To date, there are only a few systems and materials available for the production of functional-quality components hindering the introduction of this free-forming technique in the device industry. Fig. 1 shows a list of commercially available AM techniques applicable to functional materials.

While many technologies are possible for 3D printing, the most common one is called Extrusion Free Forming (EFF) or Fused Deposition Modeling (FDM), Fig. 2(a), developed and patented by S. Scott Crump in 1989. It creates complex objects from molten plastic extruded through a nozzle. The plastic filament (or even a metal wire) is wound on a coil and unreeled to supply material to the extrusion nozzle, while the nozzle or the object (or both) is moved along three axes by a computer-controlled mechanism. Material hardening takes place immediately after extrusion. For ceramic applications, FDM is based on the continuous deposition of extruded ceramic pastes to build up 3D structures.[11] Its low cost, high speed and large size capabilities are the main advantages of this technique although an intrinsic limited accuracy and surface finishing (due to the inertia of the extruder) and a reduced number of ceramic feedstock materials available still limit its applicability in many sectors. FDM of ceramics and composites is still the primary object of academic research although significant advances in omnidirectional printing of metals could be shortly adopted.[13]

A relevant AM technology is stereolithography (SLA), Fig. 2(b), where pastes containing photosensitive resins are selectively cured layer by layer. SLA can be applied to multiple materials, including ceramics and composites. It has proved to be an excellent method for fabricating fully-dense structural ceramics with high resolution and excellent surface finish.[14] However, SLA shows a strong limitation in multi-material deposition that clearly limits its applicability in multi-component devices.

Another 3D printing approach is the selective fusing of materials in a granular bed, known as selective laser sintering (SLS), Fig. 2(c). The technique fuses parts of the layer, and then moves the working area downwards, adding another layer of granules and repeating the process until the piece has built up. This process uses the unfused media to support overhangs and thin walls in the part being produced, which reduces the need for temporary auxiliary supports for the piece. A laser is typically used to sinter the media into a solid. When applied to metals and oxides with high temperature melting points, such as refractory materials, strong limitations appear. Derived densification problems combined with crack formation related to poor thermal shock resistance of ceramics become then major challenges of the SLS method.[15]

One more method is three-dimensional inkjet printing, Fig. 2(d and e). The printer creates the model one layer at a time by spreading a layer of powder[16] (plaster, resins, *etc.*) and printing a binder in the cross-section of the part using an inkjet-like process. This is repeated until every layer has been printed. The 3D inkjet printing is typically divided into direct inkjet printing (DIP) and indirect inkjet printing (IIP). DIP deposits a well-dispersed ceramic suspension *via* inkjet.[17] This is particularly appropriate to control the composition, microstructure and properties all along the component. However, the highly diluted inks usually employed in DIP slowdown the fabrication of bulky structural parts and limit the surface finish. In the case of indirect inkjet printing, parts are manufactured by distributing a binder liquid on a powder layer. The high degree of geometric freedom and elevated fabrication speed are the main advantages of this technique while the poor surface quality and difficult densification are the major limitations. The indirect printing technique is the most widely used method for commercial applications in ceramics,[18] in particular, artificial scaffolds from biocompatible ceramic materials and casting moulds.[19,20]

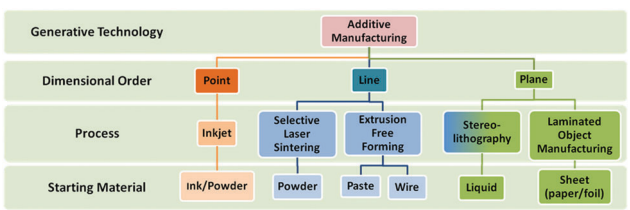

Fig. 1 Classification of the commercially available additive manufacturing methods. Adapted from ref. 11.

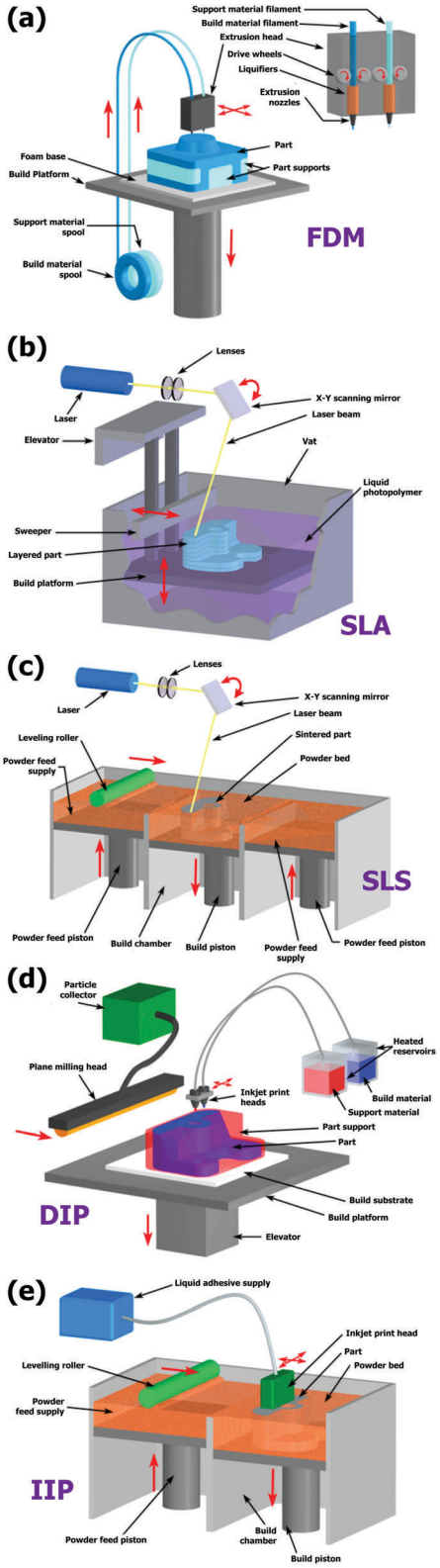

Fig. 2 3D printing systems. (a) In FDM a filament of thermoplastic is heated and extruded through a nozzle to create a 3D structure. (b) SLA uses the polymerization of a photocurable resin. (c) SLS uses a laser to fuse together powder particles. (d) DIP is based on the deposition of a well-dispersed ceramic suspension *via* inkjet. (e) IIP is a layer-by-layer process of depositing a liquid binder onto thin layers of powder to create a 3D object. Reproduced from ref. 21.

In this review, several attempts at using 3D printing technologies in the fabrication of functional components or units for the energy sector will be presented. This work is focused on dedicated efforts to increase shape complexity (by using hierarchical geometries for maximizing exposed/active surfaces), material complexity (by increasing the portfolio of printable materials and combining them into 3D printed multi-material objects) and, more importantly, functional complexity (by implementing 3D printing technologies to generate functional parts or, eventually, devices). The paper is organized by energy topics in order to focus the attention on the solutions provided by 3D printing for each particular application, Table 1.

2. Solid oxide fuel/electrolysis cells

Solid oxide fuel/electrolysis cells and stacks are geometrically complex multi-material devices based on functional ceramics. According to a recent report,[22] more than one hundred steps are required to fabricate a complete SOFC stack using traditional manufacturing processes (tape casting, punching, screen-printing, laminating, stacking or firing). This huge number of steps, some of them requiring manual input, makes the fabrication of these devices a very complex task with low reliability and complicated design for manufacturing directly associated with a long time to market. Moreover, the use of these multi-step ceramic manufacturing techniques strongly affects the reliability and durability of SOFC systems since multiple joints and seals are present in the final device. Due to these intrinsic limitations, the SOFC industry stopped pursuing highly desirable custom-designed products to promote a cost-effective concept called "mass customization" based on the combination of standard mass-produced core planar SOFC modules (US Department of Energy's Solid State Energy Conversion Alliance, SECA),[23,24] which, in the end hindered commercialization in heterogeneous sectors such as the commercial segment.

In this context, the implementation of innovative single step fabrication techniques such as 3D printing of ceramics would be crucial to overcome major limitations and reliability issues of conventional manufacturing of SOFCs while improving their durability and specific power per unit mass and volume. More specifically, 3D printing of SOFCs would allow simplification of the fabrication process, an increase of the SOFC design flexibility (allowing high-pressure joint-less monolithic systems with embedded fluidics and current collection), a reduction of the initial investment and fabrication cost together with a shorter time-to-market and, last but not least, a reduction of (waste) material and energy consumption.

Despite the evident interest of these additive manufacturing techniques for SOFC applications, the topic remained almost unexplored until the recent publication of a series of pioneering studies fully focused on addressing the lack of knowledge on 3D printing of functional ceramics of interest for SOFCs (see Table 2). They include complete details on the fabrication and electrochemical performance of the State-of-the-Art (SoA) materials for SOFC electrolytes and oxygen and fuel electrodes,[25] namely, zirconia-based

Table 1 Advantages and disadvantages of each 3D printing method, material requirements and energy applications

3D printing method/typical material requirements	Advantages/disadvantages	Energy application
FDM Thermoplastic filaments with solid loading above 40 wt% (grain size 1–5 μm)	• Cost-effective method • Printed object easily removed • Dense and porous structures can be produced after a firing process • Not good for small features, details and thin walls • Repeatability issues: warping, misalignment of layers, shifting of layers • Layer thickness of 100 μm • Postprocessing required (firing to remove organic components) • Poor mechanical properties of printed parts	Fabrication of micro-reactors (gas capture, gas separation, water purification, *etc.*) Solar concentrators Components for solid oxide fuel cells
SLA Highly viscous photocurable pastes with or w/o solid loading (>50 vol% and grain size 0.5–5 μm) Accepts pore formers	• High vertical and lateral resolution (10–25 μm) • Porous or dense materials can be printed • High surface finish • Ceramic paste acts as an integrated support structure • Large range of material options • Post-processing required (cleaning samples and firing to remove organic components) • Reusing not printed material can be difficult • Difficult to implement multi-material options • Excellent mechanical properties of printed parts	Microcell concentration PV array Fabrication of micro-reactors (gas capture, gas separation, water purification, *etc.*) Components for solid oxide fuel cells
SLS Low-to-medium melting temperature metals in powder form (grain size 0.3–10 μm)	• Mostly no post processing is required • High mechanical stability • No printed material can be reused • Powder acts as an integrated support structure • Expensive equipment • Layer thickness of 100 μm • Relatively slow speed • Finishing is dependent on powder grain size • Good mechanical properties of printed parts	Metal-supporting layer for SOFCs and metallic membranes Fabrication of complex metallic micro-reactors
DIP Highly diluted and stable inks of nanoparticles (solid concentration <5 vol% and grain size of 10–50 nm) Accepts pore formers	• High resolution layers, 1 to 10 μm • Low waste by directly printing final patterns • Allows for multiple material parts • High reproducible structures • Can be used to cover highly porous structures with a dense layer • Printing heads prone to clogging • Needs drying steps between layers • Slow for growing high aspect ratio 3D structures • Poor mechanical properties of printed parts	Components for SOFCs Components for batteries and capacitors Components for solar cells
IIP Inorganic powders with grains sizes around 50 μm	• No printed material can be reused • Powder acts as an integrated support structure • High printing velocity • Printed objects may need post-processing (hardening) • Low resolution up to 100 μm • Finishing is dependent on powder grain size • Poor mechanical properties of printed parts	Fabrication of micro-reactors (gas capture, gas separation, water purification, *etc.*)

and ceria-based electrolytes and different NiO-based and lanthanum strontium manganite, LSM-, and lanthanum strontium cobalt ferrite, LSCF-based electrodes, as well as different strategies for improving their respective interfaces.[26,27]

2.1. Dense thin electrolytes

Dense electrolytes operating at intermediate temperatures (<800 °C) are required to increase the power density of SOFC systems. However, the SoA electrolyte materials for SOFCs show low ionic conductivity. Therefore, reducing the thickness of the electrolyte layer is an extended strategy[28] for keeping its area specific resistance (ASR) within a reasonable range of values, namely ASR < 0.15 Ω cm^2. For the particular case of yttria-stabilized zirconia (YSZ), the electrolyte of choice for most of the currently available commercial SOFC cells, a maximum thickness of 50 μm is necessary to reach this ASR target at 800 °C.[29] Therefore, high-resolution ceramic 3D printing techniques able to fabricate dense thin layers are required for this application.

Based on previous knowledge on inkjet[30] and SLA[31] 3D printing of YSZ, developed for biomedical applications,[32] recent studies have been devoted to the fabrication of dense YSZ thick layers for working as electrolytes in SOFCs. Dense YSZ layers with a thickness below 10 μm have been deposited by inkjet printing onto different porous and dense substrates of interest for SOFCs.

Table 2 Cell outputs from solid oxide fuel cells fabricated totally or partially by 3D printing. (Blue text was employed to indicate the layers deposited by 3D printing technologies)

Support/printing method	Multilayer SOFC structure	OCV (V); PPD (W cm^{-2})	T (°C)	Ref.
Anode/inkjet	NiO-3YSZ/NiO-8YSZ/YSZ/LSM-YSZ/LSM	1.15; 1500	800	37
Anode/inkjet	NiO-YSZ/YSZ/LSM	1.05; 860	800	36
	NiO-YSZ/YSZ/SDC/BSCF	1.10; 1040	750	
Anode/inkjet	NiO-YSZ/YSZ/SDC/SDC-SSC	1.10; 940	750	49
Anode/inkjet	NiO–CGO/CGO/LSCF–CGO/LSCF	0.94; 710	600	50
Anode/inkjet	NiO-YSZ/NiO-YSZ/YSZ/CGO/LSCF	1.04; 377	600	48
Anode/inkjet	NiO-YSZ/NiO-YSZ/YSZ/LSM-YSZ/LSM	1.10; 500	850	33
Electrolyte/inkjet	NiO-YSZ-BZY/ScSZ/LSM	1.12; 790	900	53
Anode/AJP	NiO-YSZ/YSZ/LSM-YSZ/LSM	1.10; 440	850	52
	NiO-YSZ/YSZ/CGO/LSCF	1.18; 610	800	
Anode/inkjet	NiO-YSZ/NiO-YSZ/YSZ/LSM-YSZ/LSM	1.10; 460	850	47

Sukeshini *et al.*,[33,34] Tomov *et al.*[35] and Li *et al.*[36] deposited YSZ directly on tape cast and pre-sintered NiO-YSZ cermet substrates typically used in anode-supported SOFCs. Full SOFCs based on these inkjet-printed electrolytes were fabricated in all cases showing excellent open circuit voltages (OCVs) operating under hydrogen at 800 °C, OCV = 1.1, 1.01 and 1.05 V, respectively. These values indicate that the printed electrolytes were gas-tight layers suitable for producing high-power SOFCs.

Large area inkjet printing of even thinner YSZ layers is also possible as presented by Esposito *et al.*[37] In this work, Fig. 3, strikingly thin gas-tight 1.2 μm-thick YSZ electrolyte layers of 16 cm^2 were deposited on NiO-YSZ tape cast anode supports. Highly diluted inks (<4 vol%) based on nanometric YSZ powders (50 nm in size) were employed reducing the thickness deposited at each printing step below 300 nm while improving the printability and stability of the material. This approach allowed Esposito *et al.* to obtain negligible ASR values for the electrolyte (below 0.05 Ω cm^2) at 750 °C but close-to-theoretical open circuit voltages of OCV = 1.07–1.15 V for the full cell operating under dry hydrogen conditions.

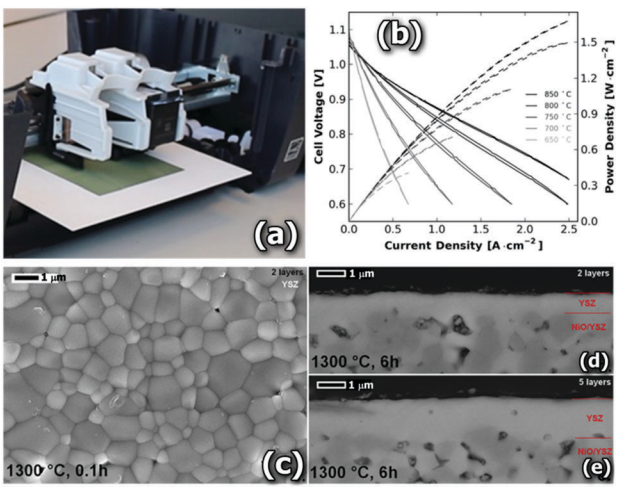

Fig. 3 (a) Modified HP 1000 ink jet printer for printing SOFC materials, reproduced from ref. 38. (b) Polarization curves recorded for the 5-layer electrolyte SOFC. (c) SEM observations of the YSZ printing of 3.7 vol% ink, sintered at 1300 °C for 6 min, and the cross-section pictures of the half cells made by (d) 2-layer and (e) 5-layer depositions after sintering at 1300 °C for 6 h. Reproduced with permission from ref. 37.

Similar studies employed inkjet printing to deposit dense thick layers of gadolinia-doped ceria (CGO), the SoA electrolyte for intermediate temperature SOFCs (IT-SOFCs),[39] onto different porous substrates. Tomov *et al.*[40] printed uniform coatings of porous NiO–CGO anodes and dense CGO electrolytes with thicknesses below 15 μm onto highly porous (>40%) metal substrates based on stainless steel. The capability of covering porous substrates was also proved by Wang *et al.*[41] and El-Toni *et al.*[42] by depositing dense CGO layers with thickness below 10 μm using NiO-YSZ and LSM porous substrates, respectively. The successful deposition of dense electrolytes onto porous substrates opens the possibility of using this 3D printing technology for the fabrication of all-type standard planar configurations including anodes, cathodes and, especially interesting, low-cost metal-supported SOFCs.[43]

Solid oxide cells not supported in the electrolyte usually suffer from deleterious long sintering times and excess sintering of the substrate, particularly for metal-supported cells, due to the high temperature required for a full densification of the SoA electrolytes. A strategy for the reduction of these elevated sintering temperatures is the substitution of inks based on stable colloidal solutions of ceramic particles by precursor-based inks. Wang *et al.*[44] showed that direct inkjet printing of sol–gel precursors of CGO allows producing thin, crack-free and dense layers at temperatures as low as 1000 °C (*vs.* typically required temperatures of 1400–1500 °C). With this approach, Wang *et al.* were able to deposit continuous coatings of CGO thinner than 10 μm on NiO-YSZ cermet substrates demonstrating the ability of inkjet printing for the fabrication of SOFC electrolytes by a cost-effective and less-energy intensive chemical route.

2.2. High performing porous electrodes and functional layers

The control of the microstructure of the electrodes and the quality of the interfaces between the electrodes and electrolyte is crucial for the performance of a solid oxide cell.[45] Among other parameters, the processing method should be able to control and tune the thickness, composition, porosity and homogeneity of the electrode or electrode functional layers. Unfair advantages characteristic of 3D printing technologies

such as the implementation of complexity at the materials, hierarchical and functional levels[46] perfectly match these requirements of the SOFC technology.

Inkjet printing allows systematically altering a number of parameters to achieve the required control of the thickness and microstructure. There are several publications available in the literature on the fabrication of tailored SOFC electrodes, both anode and cathode, by inkjet printing. Sukeshini *et al.*[33,47] were able to tailor the microstructure of SOFC cathode layers of LSM by altering the rheological property of the inks (solid loading) and the printing parameters (platen temperature or number of passes), finally obtaining similar electrochemical behavior to that for conventionally prepared cathodes. Han *et al.*[48] used inkjet printing machines to deposit lanthanum strontium cobalt ferrite (LSCF) cathodes observing that the pore size control of the deposited layer can be adjusted by using the grayscale, *i.e.* controlling the amount of ink ejection, in the printing image. Similarly, Li *et al.*[49] devoted a specific study to the control of porosity by the introduction of up to 10 wt% pore former in the ink formulation of a cathode composite (samaria-doped ceria and samarium strontium cobalt oxide, SDC/SSC). The introduction of the pore former yielded polarization comparable to the ones obtained for commercial pastes of the same material.

Yashiro *et al.*[50] and Li *et al.*[36] reported the use of inkjet printing for the fabrication of intermediate or buffering layers for SOFCs. In particular, Yashiro *et al.*[50] fabricated LSCF–CGO cathode functional layers with a large quantity of triple phase boundaries (TPBs). Precise control of the thickness and composition of the layer was easily achieved by variation of the number of printing cycles and adjustment of the LSCF : CGO ratio in the printed ink, respectively. This tunability of the thickness and composition of the functional layer resulted in an over 30% performance enhancement of SOFC cells including a 3 μm-thick functional layer compared to reference cells (Ni–CGO/CGO/CGO–LSCF). Li *et al.*[36] likewise fabricated dense and rough 2 μm-thick buffering layers of SDC that allowed the use of high-performing cathode materials typically reacting with YSZ such as $Ba_{0.5}Sr_{0.5}Co_{0.8}Fe_{0.2}O_{3-\delta}$. Pursuing the same idea of improving the performance of different interfaces, functionally graded anodes[51] and cathodes[52] were fabricated by Aerosol Jet Printing (AJP) by Sukeshini *et al.* obtaining highly reproducible microstructures and performance improvement.

Alternatively, inkjet printing has been employed in the SOFC context to substitute conventional manual infiltration of solutions containing suitable catalyst materials on thermally stable scaffolds. Shimada *et al.*[53] finely controlled the distribution of yttrium-doped zirconate (BZY) in pre-sintered Ni-YSZ SOFC anodes by inkjet printing infiltration solutions based on the corresponding metal chlorides. Similarly, Da'as *et al.*[54] recently presented the use of inkjet printing for the fabrication of hierarchically microstructured SOFC cathodes by infiltration of aqueous solutions of metal nitrates for impregnation of LSM into YSZ porous bodies. Dudek *et al.*[55] also proved that it is possible to carry out both the scaffold fabrication and the infiltration process by inkjet printing for application in direct carbon SOFCs (DC-SOFCs). All in all, this and previous studies indicate the feasibility of the inkjet printing process to fabricate the desired complex hierarchical, compositional and microstructural functional multi-layers that enhance the electrode performance in SOFCs.

2.3. Performance of full solid oxide fuel cells

A collection of SOFC performance results for cells including single or multiple 3D printed layers is presented in the literature. Table 2 compares the cell outputs of selected studies indicating the layers fabricated with 3D printing techniques. The high quality of inkjet-printed electrolytes for solid oxide fuel cells is totally proved after the remarkable peak power density (PPD) of 1.5 W cm^{-2} at 800 °C recently reported by Esposito *et al.*[37] for large-area YSZ electrolytes and the maximum power densities of 1040 mW cm^{-2} at 750 °C reported by Li *et al.*[36] for YSZ/SDC bi-layer electrolytes. In the same way, optimized cathode composites suitable for SOFC applications were achieved as shown by Li *et al.*[49] for SDC/SSC composites that yielded PPDs of 940 mW cm^{-2} at 750 °C and by Yashiro *et al.*[50] that obtained maximum outputs of 710 mW cm^{-2} at 600 °C for inkjet-printed LSCF/CGO layers. The benefits of the infiltration of anode supports by direct printing of catalyst or co-catalyst materials was also proved at a cell level by Shimada *et al.*[53] obtaining PPDs of 790 mW cm^{-2} at 900 °C for BZY-infiltrated Ni/YSZ anodes.

Finally, it is important to remark here some pioneering studies by Sukeshini *et al.*[33,47] devoted to configuring complete SOFC cells by direct printing of all non-supported layers. Full SOFC cells were fabricated by printing NiO-YSZ anode functional layers, YSZ electrolyte layers, LSM-YSZ cathode functional layers and LSM cathode current collector layers on a NiO-YSZ pre-sintered support. The optimized cells exhibited a close-to-theoretical open circuit voltage of 1.1 V and a reasonable peak power density of 460 mW cm^{-2} at 850 °C for hydrogen.

2.4. Future prospects

After confirming the feasibility of producing high performing functional layers and even complete planar SOFCs by direct printing, these novel fabrication techniques should be explored to generate advanced 3D configurations at the cell and stack level able to provide high specific power per unit mass and volume. This will probably require the fabrication of high-aspect-ratio architectures difficult to achieve with the inkjet printing-based technology currently employed for SOFCs. In this direction, some interesting studies have been devoted to exploring the use of alternative 3D printing technologies for SOFC applications such as Meniscus-confined electrodeposition (MCED),[56] Fig. 4, stereolithography[57] or extrusion,[58,59] more suitable for fabricating large volumes. However, the difficult implementation of multi-material capabilities in SLA and the poor resolution in the microscale characteristics of the extrusion methods, will be major limitations for straightforwardly employing these techniques to fabricate complex SOFC architectures. It is clear that further work is needed to develop hybrid 3D printers able to combine unique features of different printing techniques to build up high-aspect-ratio multi-material solid oxide cells with the required high accuracy on the microscale.

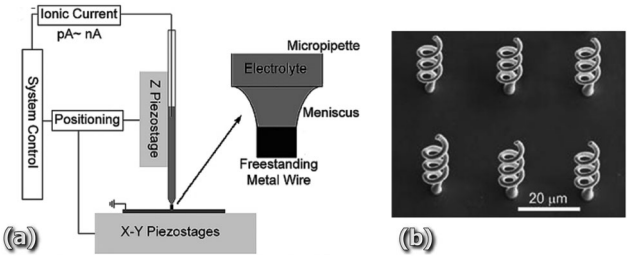

Fig. 4 (a) Schematic of a basic deposition MCED set-up composed of piezo stages and the electrolyte containing micropipette and the dispensing nozzle and (b) SEM image of six identical microstructures fabricated using a copper-based electrolyte. Reproduced from ref. 56 with permission from The Royal Society of Chemistry.

In addition, in order to be able to print the single repeating units that form full stacks, renewed efforts should be focused on extending the list of printable materials of interest for SOFCs, at least, to (ceramic) interconnects. This will allow target architectures to be reached consisting of support-less or joint-less stack configurations only achievable by single deposition and sintering steps.[60]

3. Batteries and supercapacitors

Li-batteries are the most widely used power systems for portable applications with a global market of over $20 billion in 2015. The intensive R + D activities in the last few decades have led to highly efficient devices, in many cases close to the maximum theoretical performances dictated by material choice. Processing is also undergoing phenomenal progress in the search for highly efficient commercial devices *via* the use of flexible batteries, taking advantage of materials with very high surface areas.[61]

3.1. Three-dimensional materials and devices

The concept of using 3D materials for energy applications has been explored over the last 15 years. Indeed, battery performance can be greatly enhanced by reconfiguring conventional materials in 2D batteries or supercapacitors into 3D frameworks.[62] Such an approach results in the maximisation of both power and energy density while the ionic paths remain short.[63] A clear example of that concept is the development of materials exhibiting hierarchical porosity[64–66] or nanostructures.[67]

There are a large number of examples in the literature reporting progress in the production of 3D materials for Li-batteries and/or ultracapacitors,[68–71] including graphene printed out of specially designed inks,[72–75] however this concept is still at a very early stage regarding 3D processing despite the promise of very high theoretical efficiencies.[76]

Kohlmeyer *et al.*[75] established a universal approach to develop 3D printable and free-standing electrodes with embedded current collectors for Li-ion batteries, Fig. 5. They used direct ink write printing of composite electrodes made of active material ($Li_4Ti_5O_{12}$, $LiFePO_4$ or $LiCoO_2$), carbon nanofibers as a conductive additive and a polymer based on poly(vinylidene fluoride) (PVDF).

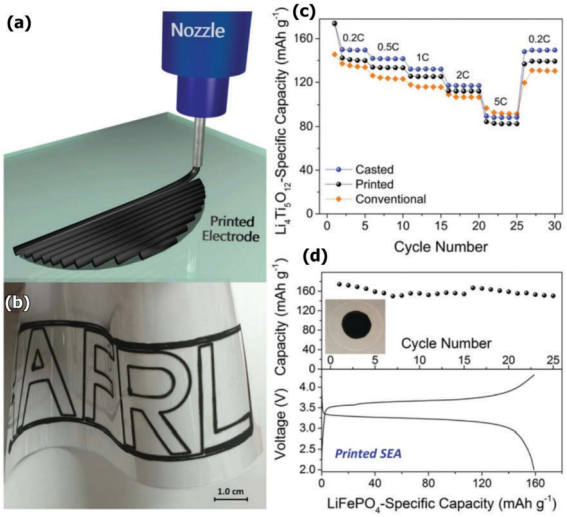

Fig. 5 Printing of 40/40/20 active/CNF/PVDF composite electrodes. (a) Schematic illustration of the filamentary printing process. (b) Rate performance of printed and cast composites and a conventional $Li_4Ti_5O_{12}$ electrode on copper. (c) Photograph of a complex filamentary printed design prepared using cathode ink on transparent paper. (d) Cycle performance and charge/discharge profile (0.05C). Reproduced from ref. 75 with permission from The Royal Society of Chemistry.

Nevertheless, efforts to assemble 3D batteries/capacitors are ever-growing and a clear example of that is the development of the so-called interdigitated batteries and capacitors that require the use of lithographic methods or micromachining as was the case for one of the first C-electrodes developed by Ranganathan *et al.*[77] Further progress has been recently reported by Liu *et al.* with the fabrication of metallic scaffolds *via* direct melting laser sintering that may be further functionalized to serve as pseudocapacitors.[78]

Using an analogous approach as is the case of 3D holographic lithography, Pikul *et al.*[79] produced Li microbatteries with power densities exceeding those of the best supercapacitors[80] (*e.g.* 7.4 mW cm^{-2} mm^{-1}), Fig. 6, and energy densities in the same range (*e.g.* 15 mW h cm^{-2} mm^{-1}).[80–82]

The same group[83] reported the fabrication of Li-ion microbatteries which combine high energy densities (6.5 mW h cm^{-2} mm^{-1}) and supercapacitor-like power (up to 3600 mW cm^{-2} mm^{-1}) and retain at least 80% of the initial capacity after 100 cycles in a range of discharge rates (5C–20C). The procedure consists of the production of a thick 3D framework of SU-8 (an epoxy-based photoresist) and further infiltration with another photoresist that contains the battery materials.

Recently, a fairly similar strategy has been developed by Nyström *et al.*[84] to produce 3D supercapacitors, though it may be extended to batteries as well. In the layer by layer assembly, the entire power system self-assembles inside aerogels with perfect control of the thickness in the range of nanometers. The resulting supercapacitors exhibited capacitances of 25 F g^{-1} and were stable after several hundreds of cycles.

A closer example of conventional 3D-printing techniques is the fabrication of interdigitated supercapacitors made out of graphene *via* micro-extrusion.[85] The supercapacitors prepared

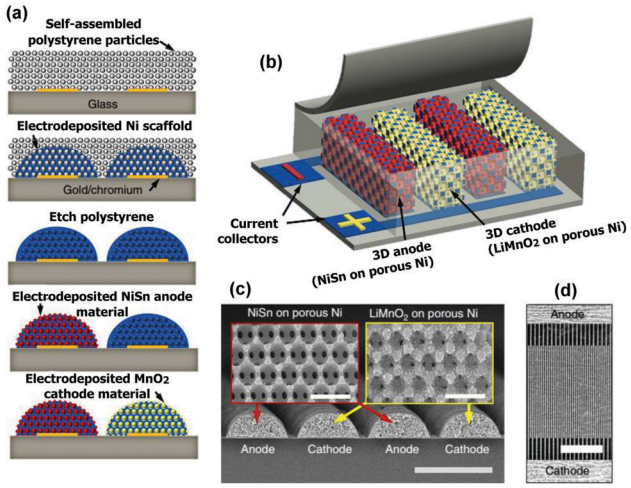

Fig. 6 Fabrication of high performance 3D Li-ion microbatteries. (a) Schematic of the fabrication process where the nickel scaffold defines that the battery architecture and the active materials are electrodeposited onto the nickel scaffold. (b) Microbattery design. (c) Scanning electron microscopy (SEM) cross-section of the interdigitated electrodes spanning two periods. Scale bars, 50 μm and 1 μm in the insets. (d) A top-down SEM image of the interdigitated electrodes. Scale bar, 500 μm. Reproduced from ref. 79.

using an XYZ stage coupled to a syringe-pump rendered modest capacitance although they exhibit fairly high stability after several thousands of cycles.

Ink-jet printing is another widely used procedure to print mostly battery/capacitor components,[86–91] but the assembly of the battery using 3D printing technologies is not trivial at all and indeed there are just a few reports in the literature regarding the fabrication of complete 3D-printed batteries. One of the first examples was reported by Ho *et al.*, who were able to fabricate a Zn–Ag battery exhibiting up to 60% capacity increase compared to conventional planar designs.[92]

Recently, Sun *et al.*[61] reported the fabrication of entire power systems *via* ink-jet printing, based on $La_4Ti_5O_{14}$ and $LiFePO_4$ electrodes, stacking 8 and 16 layers, Fig. 7, delivering up to 1.5 mA h cm^{-2} at a stable 1.8 V at discharge rates below 5C. The performance is relatively low compared to the equivalent conventional batteries, probably due to long conducting paths between the electrodes, and also the packaged batteries did not exhibit long-term cyclability. Nevertheless, these results constitute a clear proof of concept that highly efficient microbatteries may be produced *via* 3D-printing.

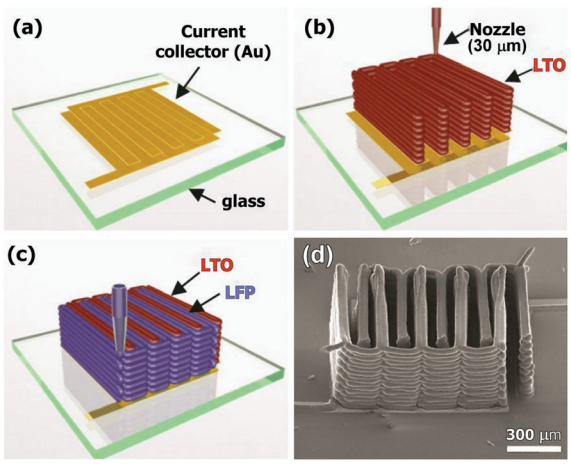

Fig. 7 (a) Schematic illustration of a 3D interdigitated microbattery fabricated on (a) a gold current collector by printing $Li_4Ti_5O_{12}$ (b) and (c) $LiFePO_4$ inks through 30 μm nozzles, followed by sintering. (d) SEM image of the 3D microbattery. Reproduced from ref. 95.

Although they cannot be considered as additive manufacturing strictly speaking, there are similar approaches to fabricate printable solid-state batteries by using stencil printing. Stencil printing has been used in the production of transparent flexible Li-batteries.[93] This approach initially led to fairly modest electrochemical efficiencies, *e.g.* current densities of 10 A cm^{-2} at 2 mV s^{-1}, which is one order of magnitude lower than in conventional Li-batteries, but already showing good capacity retention. Indeed, the refinement of the technique and the electrode material choice rendered better results.[94] Capacity retention of up to 90% after 30 cycles has been reported for flexible printed Li-batteries, with the additional advantage of almost free-form fabrication.

3.2. Future prospects

The fabrication of working devices *via* ink-jet constitutes a clear example of the potential use of these technologies for energy storage systems. To date, most of the work reported relates to individual components and therefore one would expect more examples of high-aspect ratio architectures in the near future. Further progress is required in alternative 3D printing techniques such as SLA or even FDM to produce larger systems as ink-jet printed devices are somewhat restricted to microbatteries. However that would imply a great deal of effort to increase the number of printable materials as nowadays the choice is rather limited. If that is achieved, printing multimaterial devices *via* SLA would be a good choice, though this technology is not mature yet as mentioned above and may require novel printers. FDM could be used to fabricate prototypes.[96] Although the resolution would be clearly lower and may not be suitable for commercial devices, novel architectures could be produced as a proof of concept.

The development of Li-ion polymer conductors is perhaps one of the research fields where 3D printing may play a very relevant role in the near future in the search for highly reproducible flexible batteries, particularly with the development of roll-to-roll systems described in Section 4.

4. Solar energy applications

4.1. Flexible solar cells and modules

3D printing has been very recently introduced in several solar applications, promising to revolutionize photovoltaic (PV) cells and solar panel manufacturing and efficiency. 3D printing will ensure lower production costs of flexible and lighter solar panels for implementation on buildings, indoor applications, wearable hi-tech clothing and portable electronics.

High-throughput large-scale roll-to-roll fabrication of PV cells on flexible substrates, such as transparent plastics and

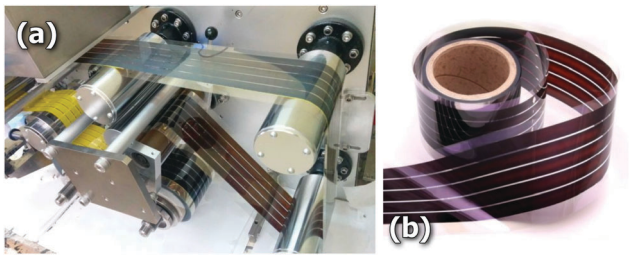

Fig. 8 (a) A 3D-printer based slot-die coater as a lab-to-fab translation tool for solution-processed solar cells, (b) aimed at potential use in large-scale roll-to-roll printing of perovskite solar cells. Reproduced with permission from ref. 107.

metallic foils, seems to be one of the most promising uses of 3D-printing technology in the PV sector. F. C. Krebs[97] recently reviewed the most relevant coating and printing techniques in the field of polymer solar cells concluding that techniques such as gravure coating knife-over-edge and slot-die are more likely to gain dominance together with inkjet printing for complex patterns and advanced devices. In this sense, Vak *et al.*[98,99] have recently reported the use of a 3D printer assisted slot-die coater, Fig. 8, for scalable fabrication of printed perovskite solar cells with ~11.6% efficiency and solar cell modules with ~4.6% efficiency built on large-area ITO glass substrates (>48 cm^2). Although rigid substrates were employed by Vack and coworkers, such low temperature technologies can be easily extended to flexible substrates making 3D printing a potential lab-to-fab tool for solution-processed solar cells.[100]

An alternative to flexible organic cells is based on arrays of ultra-thin semitransparent solar microcells, which can reach a similar efficiency to conventional solar panels.[101] This type of panel requires flexible interconnects, *i.e.* flexible front electrodes. In general, front electrodes are one of the major challenges for Si solar cells and 3D printing has been extensively used to fabricate silver based electrodes.[102–104]

Ahn *et al.*[106] were able to fabricate flexible, stretchable, and spanning silver microelectrodes using a 3-axis micropositioning stage coupled to a micronozzle (see Fig. 9). Similar bridging capabilities were also shown for Sn-doped indium oxide (ITO), a typical transparent conductor, using the same 3D printing technology.[106] The striking omnidirectionality of these flexible microelectrodes opens new avenues for designing complex three-dimensional photovoltaic structures.

In this regard, researchers at the Massachusetts Institute of Technology carried out a computational study to optimize arbitrarily shaped three dimensional photovoltaic (3DPV) structures to maximize the energy production by using a genetic algorithm[108,109] proving that properly designed solar panels could be more efficient than flat solar panels by significantly extending the amount of solar radiation absorbed by the cells without sun tracking. In detail, Bernardi *et al.*[109] mounted commercially available Si solar cells onto 3D-printed plastic frames with optimized geometries demonstrating energy densities per projected area (kW h m^{-2}) higher than flat stationary panels by a factor between 2 and 20 and an enhancement factor in energy density of 1.5 to 4 times. Beyond 3D-printed plastic

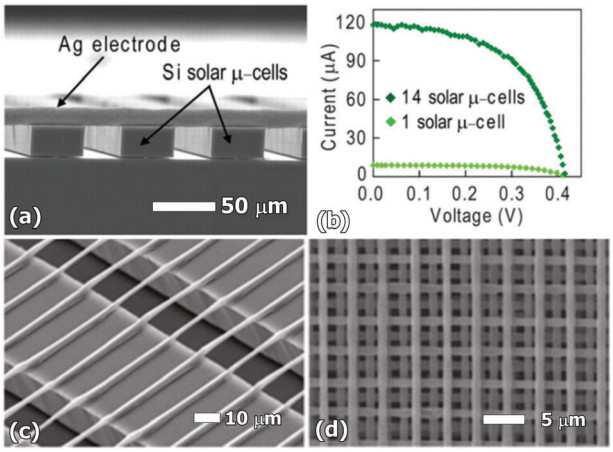

Fig. 9 (a) Spanning silver microelectrodes deposited by 3D printing to connect an unplanarized Si solar micro-cell array; (b) current (*I*)–voltage (*V*) response of an individual silicon solar microcell and a 14-microcell array connected by silver microelectrodes; (c) spanning ITO microelectrodes printed on Si ribbons; and (d) 3D structure of ITO strips. Reproduced from ref. 105 and 106 with permission from The Royal Society of Chemistry.

frames, these simple or even more complex and efficient origami-like 3D geometries require the use of inexpensive and customized flexible cells and stretchable interconnects, which are currently under development by the 3D printing community, as previously shown in this section. 3D printing is therefore a firm candidate to enable a revolution in the PV sector based on 3DPV.

4.2. Solar concentrators

With respect to 3D-printing fabrication of functional parts and devices for solar cell applications, the very recent demonstration of 3D-printed concentration arrays for external light trapping on thin film solar cells is of increasing interest. The external light trap mechanism relies on focusing the sunlight through a small aperture of a parabolic concentrator before reaching the PV cell, and a spacer, which redirects the photons that are reflected upwards by the solar cell back towards the solar cell.[110,111] Due to this retro-reflection, light passes through the solar cell multiple times giving rise to a noticeable broadband absorption enhancement and higher power conversion efficiency.[112]

External light trapping using solar concentrators (or parabolic mirrors) leaves the solar cell properties intact as it does not internally modify the cell and therefore can benefit from the high quality of thin film solar cells. In this sense, van Dijk and co-workers[111] have recently presented an optimization analysis of external light trapping, with the fabrication of 3D-printed external light traps with square, hexagonal and circular compound parabolic concentrator arrays, Fig. 10. They demonstrated that 3D-printed traps, made of smoothened, silver-coated thermoplastic, placed on top of an organic solar cell resulted in a significant enhancement of the external quantum efficiency (EQE), such as a 15–27% efficiency enhancement for crystalline silicon, thin film nanocrystalline silicon and organic solar cells. In detail, an improvement up to 16% of the EQE has been reported with a 3D-printed circular solar concentrator implemented on a flat organic solar cell.

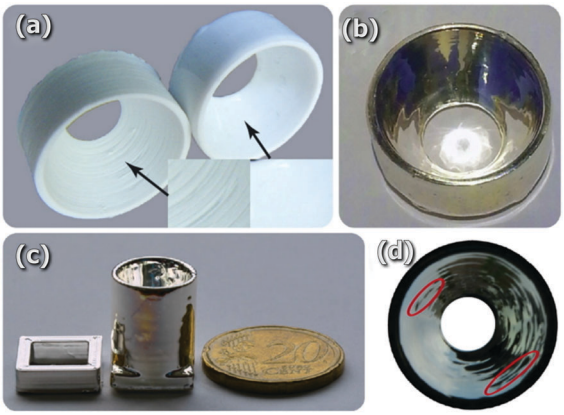

Fig. 10 (a) A 3D-printed compound parabolic solar concentrator (CPC) before and after chemical smoothening, the insets show the enlarged surface. (b) The silver-coated CPC with a focal ring of sunlight at the center. (c) The separated cage and CPC that can be combined to an external light trap. (d) View of the CPC from the entrance side, showing the reflection in the parabolic curve. Two wrinkles in the concentrator are encircled in red. Reproduced with permission from ref. 111.

Furthermore, concentration integrated optics developed for maximizing the conversion efficiency of PV technology as described above can be also used for attaining high power densities required for the modification of the solar spectrum to achieve a better match with the wavelength dependent conversion efficiency of the PV device, in the so-called "Third Generation Solar Cells", also known as up-conversion solar cells (UCSCs) or up-conversion photovoltaics (UC-PV).[113] In up-conversion (UC) luminescence processes two low energy (sub-band gap) photons are combined to one high energy photon. This conversion allows the harvested solar spectrum to be widened in existing solar cells by independent optimization of the solar cell and the spectral up-converter materials (lanthanides, actinides and transition metals).[114] In this line, Arnaoutakis and co-workers[115,116] have successfully integrated concentrating optics into up-conversion PV devices, Fig. 11. Such a complex device approach is very convenient for employing 3D-printing technologies since focusing optics and polymer-based coatings films have been successfully carried out in recent years by using multi-material stereo-lithography (SLA).[117] Recently, a modified UV-inkjet printing technology (Printoptical©[118]) has been developed to fabricate high-quality plastic optics. This technology has been already applied to solar applications overcoming typical surface quality problems derived from 3D printing, in particular, Printoptical© was used by Price *et al.*[119] to fabricate a small-scale microcell concentration PV array. The combination of this (or a similar) technology with recent advances in the development of SLA printable spectral converting rare-earth doped organic resins[120,121] opens the possibility of directly fabricating integrated up-conversion and focusing optics by 3D printing for a new generation of enhanced solar cells.

4.3. Future prospects

Printed electronics is currently evolving toward more complex applications including multi-layer flexible solar cells (organic/inorganic) and complex 3D solar collectors. This low-cost and large-area 3D printing process will allow a breakthrough in PV manufacturing, probably enabling the expected revolution of three-dimensional photovoltaic structures that are highly efficient even in the absence of sun tracking. Before this will take place, major advances in 3D printing of flexible (contact) materials and high-quality optics are still required together with the need of developing new printable inks of active materials for growing multilayer devices.

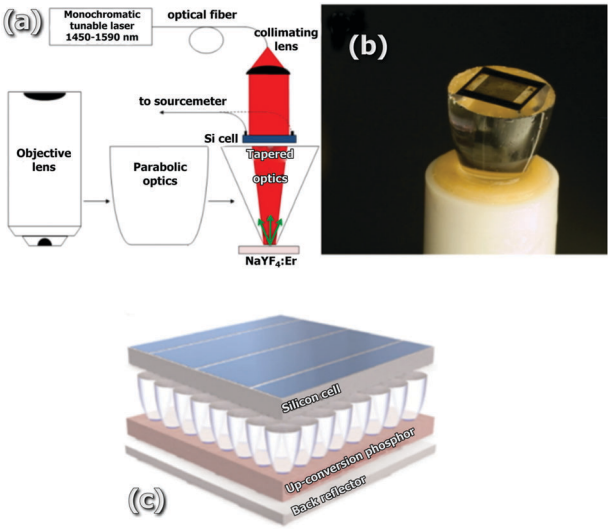

Fig. 11 (a) Schematic of the UC-PV device with integrated optics behind the solar cell. (b) Details of one of the parabolic concentrators used with a bifacial silicon solar cell attached. The UC phosphor is attached on the exit aperture of the parabolic concentrator. (c) Artistic impression of the UC-SC with a regular two-dimensional array of integrated CPC optics. The gaps between the layers are only for illustrative reasons. Reproduced with permission from ref. 115 and 116.

In the near future, the development of multi-material 3D printing systems able to integrate focusing optics, coatings and embedded luminescent–polymer composites for the fabrication of new generations of advanced solar cells based on up-conversion photovoltaics or even Luminescent Solar Concentrators (LSCs) will also be of particular interest. LSCs mainly consist of highly transparent plastic plates, comprising high quantum efficiency luminescent species, for absorbing incident light and re-emitting at a red-shifted wavelength directly allowing concentrated and wave-guided converted radiation.[122] These LSCs could be a cheap alternative to silicon substrates for building integration applications.

Finally, it is also interesting to be aware of the development of environmentally sensitive materials able to actively transform configurations over time in response to external stimuli[123] since the use of shape-memory polymers in so-called 4D printing could be especially interesting for developing self-configurable, active and adaptable harvesting devices such as solar cells.[124]

5. Catalytic reactors for fuel production and CO_2 capture

Classical micro-structured catalytic reactors (MSCRs) consist of simple three-dimensional rigid structures covered by a catalyst.

These 3D structures are usually extruded and therefore are strongly limited in shape. However, tailoring geometrical features such as channel geometry, diameter, porosity and surface–volume ratio are crucial for (i) maximizing the mass and heat transfer which leads to more active and stable catalytic reactors and (ii) decreasing the generation of waste heat, thereby minimizing energy consumption and increasing production efficiency.

Different authors have reported 3D fabrication of catalyst supports based on alumina.[125–127] Although in these cases the 3D printing techniques were employed to fabricate the structural but functional material of the reactor, they showed the suitability of AM for solving problems associated with limitations in the classical fabrication of reactors. Structured internals available by 3D printing can play a very important role and allow solutions that were previously impossible.[126] The aim is an optimal integration of mass, heat and momentum transfer within a single reactor vessel.[128] Moreover, the possibility of generating an internal structure by design rather than chance, like in packed bed, monolithic- or foam-type reactors, allows a new family of micro-structured catalytic reactors with very flexible and efficient use of catalyst in the reactor volume.[129]

Exploring a higher functionality of the 3D printed reactor itself, Tubío *et al.*[130] recently reported direct 3D printing of a heterogeneous catalytic system including Al_2O_3-supported copper species. The 3D printing process enabled here the direct fabrication of a woodpile porous catalyst with excellent catalytic performance for different Ullmann reactions, Fig. 12. Complementarily, a few examples can be found in the literature where the catalyst is embedded in the printed matrix for different applications. In particular, Symes *et al.*[131] developed reactionware that included printed-in catalysts for, among other applications, photocatalysis. Similarly, the previously mentioned 3D-printed structures containing rare-earth (RE) doped up-conversion luminescent materials[120,121] (Section 4.2) were also proposed to be used in the design and fabrication of up-converting-coated vessels, photoreactors or light-guiding structures with potential direct implementation in photocatalysis and solar-to-fuel applications. In the same direction, Skorski *et al.* were able to print photocatalytic membranes based on polymer–TiO_2 nanocomposites.[132]

Finally, it is worth mentioning recent efforts towards developing 3D printed reactors for CO_2 capture and removal. Thakkar *et al.*[133] developed 3D-printed zeolite monoliths fabricated by EFF. The high zeolite loading content (>90 wt%) of the reactors (also containing small amounts of clay acting as a binder) yielded adsorption results comparable to their powder counterpart with more shape flexibility and mechanical stability. Couck *et al.*[134] recently developed a new method based on printing several layers of zeolite fibers on top of each other (Three Dimensional Fiber Deposition, 3DFD) for producing zeolite monoliths for CO_2 gas separation. The 3DFD printed monolithic structures showed good separation performance slightly below the pure powder.

This approach can be analogously replacing in the same way for the fabrication of catalytic reactors for any other process, not only for CO_2 capture: printing of a 3D inorganic/metal supporting structure, and then covering the 3D structure with a layer of catalytic/photocatalytic material typically deposited by impregnation of an aqueous solution or, direct printing of the 3D reactor with an appropriate catalytic material by FDM.

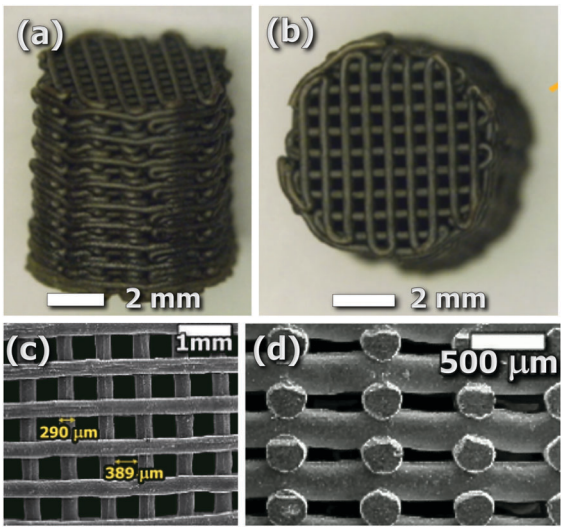

Fig. 12 (a and b) Optical images of a sintered Cu/Al_2O_3 3D structure deposited through a 410 μm nozzle. SEM images, (c) top view, (d) cross-sectional view. Reproduced from ref. 130.

5.3. Future prospects

3D printing technologies open new possibilities for tailoring catalytic reactors with different applications in the energy sector, *e.g.* heterogeneous catalysis for green fuel production, CO_2 capture or gas separation membranes. Although an evident benefit will come from the proper design of structured reactors for improving heat transfer, optimized mass transfer and good reaction performance, the highest impact of the 3D printing technology is expected to come from the direct fabrication of reactors with embedded catalysts and controlled porosity. Therefore, further efforts should be devoted to developing new printable functional composites involving key materials for catalysis together and new strategies to fine-tune the microstructure of the printed objects.

6. Conclusions

Additive manufacturing or 3D printing technologies offer unique capabilities for the fabrication of improved key devices for the energy and environmental sectors. In particular, the possibility of fine tuning shapes for increasing their exposed active surface is crucial, *i.e.* for maximizing their specific performance per unit mass and volume. The use of 3D printing technologies for the fabrication of these devices is also of special interest due to the strong manufacturing limitations of typically employed advanced materials such as ceramics or composites. For these materials, 3D printing represents a major breakthrough in shape complexity and great simplification of the design for manufacturing and fabrication processes. However, in order to benefit from the improved performance and the associated reduction of cost and waste material, further work is required to develop multi-material

3D printing systems, increase the portfolio of printable advanced materials and test the functionality of the printed pieces and devices.

Acknowledgements

This work was supported by the ''Ministerio de Economía y Competitividad'' (MINECO), grant numbers ENE2013-47826-C4-1-R, ENE2013-47826-C4-3-R, ENE2013-47826-C4-4-R and ENE2016-74889-C4-2-R (AEI/FEDER, UE). The project Cell3Ditor acknowledges the financial support of the European Union in the frame of the Horizon 2020 programme, under RIA-FCH2-JU, Grant number 700266-Cell3Ditor.

Notes and references

1 B. Utela, D. Sorti, R. Anderson and M. Ganter, *J. Manuf. Process.*, 2008, **19**, 96.
2 R. D. Farahani, M. Dubé and D. Therriault, *Adv. Mater.*, 2016, **28**, 5794.
3 Disruptive technologies: Advances that will transform life, business, and the global economy, MGI, May 2013.
4 K. Maeda and K. Domen, *J. Phys. Chem. Lett.*, 2010, **1**, 2655; M. Ni, M. K. H. Leung, D. Y. C. Leung and K. Sumathy, *Renewable Sustainable Energy Rev.*, 2007, **11**, 401.
5 A. Steinfeld, *Sol. Energy*, 2005, **78**, 603.
6 J. C. Ruiz-Morales, J. Canales-Vázquez, C. Savaniu, D. Marrero-López, W. Zhou and J. T. S. Irvine, *Nature*, 2006, **439**, 568.
7 Y. Tiana and C. Y. Zhao, *Appl. Energy*, 2013, **104**, 538.
8 H. S. Sayed Ali Hassain, Fabrication of Ceramics and Ceramic Composite Microcomponents using Soft Lithography, PhD thesis, The University of Birmingham, United Kingdom, 2010.
9 K. J. A. Brookes, *Metal Powder Report*, 2015, **70**, 68.
10 B. Y. Tay, J. R. G. Evans and M. J. Edirisinghe, *Int. Mater. Rev.*, 2003, **48**, 341.
11 N. Travitzky, A. Bonet, B. Dermeik, T. Fey, I. Filbert-Demut, L. Schlier, T. Schlordt and P. Greil, *Adv. Eng. Mater.*, 2014, **16**, 729.
12 J. Rödel, A. B. N. Kounga, M. Weissenberger-Eibl, D. Koch, A. Bierwisch, W. Rossner, M. J. Hoffmann, R. Danzer and G. Schneider, *J. Eur. Ceram. Soc.*, 2009, **29**, 1549.
13 B. Y. Ahn, E. B. Duoss, M. J. Motala, X. Guo, S. Park, Y. Xiong, J. Yoon, R. G. Nuzzo, J. A. Rogers and J. A. Lewis, *Science*, 2009, **323**, 1590; Voxel8, http://www.voxel8.com, accessed november 2016.
14 H. Wu, W. Liu, R. He, Z. Wu, Q. Jiang, X. Song, Y. Chen, L. Cheng and S. Wu, *Ceram. Int.*, 2017, **43**, 968.
15 J.-P. Kruth, P. Mercelis, J. Van Vaerenbergh, L. Froyen and M. Rombouts, *Rapid Prototyping J.*, 2005, **11**, 26.
16 P. Calvert, *Chem. Mater.*, 2001, **13**, 3299.
17 J. A. Lewis, J. E. Smay, J. Stuecker and J. Cesarano III, *J. Am. Ceram. Soc.*, 2006, **89**, 3599.
18 U. Kalsoom, P. N. Nesterenko and B. Paull, *RSC Adv.*, 2016, **6**, 60355.
19 H. N. Chia and B. M. Wu, *J. Biol. Eng.*, 2015, **9**, 1.
20 S. J. Hollister, *Nat. Mater.*, 2005, **4**, 518.
21 http://www.custompartnet.com/wu/additive-fabrication, accessed november 2016.
22 M. R. Weimar, L. A. Chick, D. W. Gotthold and G. A. Whyatt, Cost Study for Manufacturing of Solid Oxide Fuel Cell Power Systems, Pacific Northwest National Laboratory, contract DE-AC05-76RL01830, September 2013.
23 W. A. Surdoval, S. C. Singhal and G. L. McVay, The Solid State Energy Conversion Alliance (SECA). A U. S. Department of Energy initiative to promote the development of mass customized Solid Oxide Fuel Cells for low-cost power, in *Proceedings of the Seventh International Symposium on Solid Oxide Fuel Cells, PV 2001-16*, ed. H. Yokokawa and S. C. Singhal, The Electrochemical Society, Pennington, NJ, 2001, p. 53.
24 S. C. Singhal, *Solid State Ionics*, 2002, **152–153**, 405.
25 N. Mahato, A. Banerjee, A. Gupta, S. Omar and K. Balani, *Prog. Mater. Sci.*, 2015, **72**, 141.
26 J. T. S. Irvine, D. Neagu, M. C. Verbraeken, C. Chatzichristodoulou, C. Graves and M. B. Mogensen, *Nat. Energy*, 2016, **1**, 15014.
27 J.-h. Myung, D. Neagu, D. N. Miller and J. T. S. Irvine, *Nature*, 2016, **537**, 528.
28 A. Tarancón, *Energies*, 2009, **2**, 1130.
29 D. J. L. Brett, A. Atkinson, N. P. Brandon and S. J. Skinner, *Chem. Soc. Rev.*, 2008, **37**, 1568.
30 J. Ebert, E. Özkol, A. Zeichner, K. Uibel, Ö. Weiss, U. Koops, R. Telle and H. Fischer, *J. Dent. Res.*, 2009, **88**, 673.
31 F. Doreau, C. Chaput and T. Chartier, *Adv. Eng. Mater.*, 2000, **2**, 493.
32 R. G. Luthardt, M. Holzhüter and O. Sandkuhl, *J. Dent. Res.*, 2002, **81**, 487.
33 A. M. Sukeshini, R. Cummins, T. L. Reitz and R. M. Miller, *J. Am. Ceram. Soc.*, 2009, **92**, 2913.
34 D. Young, A. M. Sukeshini, R. Cummins, H. Xiao, M. Rottmayer and T. Reitz, *J. Power Sources*, 2008, **184**, 191.
35 R. I. Tomov, M. Krauz, J. Jewulski, S. C. Hopkins, J. R. Kluczowski, D. M. Glowacka and B. A. Glowacki, *J. Power Sources*, 2010, **195**, 7160.
36 C. Li, H. Shi, R. Ran, C. Su and Z. Shao, *Int. J. Hydrogen Energy*, 2013, **38**, 9310.
37 V. Esposito, C. Gadea, J. Hjelm, D. Marani, Q. Hu, K. Agersted, S. Ramousse and S. H. Jensen, *J. Power Sources*, 2015, **273**, 89.
38 http://www.energy.dtu.dk/english/news/2014/05/print-a-sofc-using-inkjet-printing?id=2a9cfee2-04cf-4a80-845c-d4ae977680d8, accessed December 2016.
39 M. Mogensen, N. M. Sammes and G. A. Tompsett, *Solid State Ionics*, 2000, **129**, 63.
40 R. I. Tomov, M. Krauz, A. Tluczek, R. Kluczowski, V. V. Krishnan, K. Balasubramanian, R. V. Kumar and B. A. Glowacki, *Mater. Renew. Sustain. Energy*, 2015, **4**, 14.
41 C. Wang, S. C. Hopkins, R. I. Tomov, R. V. Kumar and B. A. Glowacki, *J. Eur. Ceram. Soc.*, 2012, **32**, 2317.
42 A. M. El-Toni, T. Yamaguchi, S. Shimizu, Y. Fujishiro and M. Awano, *J. Am. Ceram. Soc.*, 2008, **91**, 346.
43 M. C. Tucker, *J. Power Sources*, 2010, **195**, 4570.

44 C. Wang, R. I. Tomov, R. V. Kumar and B. A. Glowacki, *J. Mater. Sci.*, 2011, **43**, 6889.
45 J. C. Ruiz-Morales, D. Marrero-López, M. Gálvez-Sánchez, J. Canales-Vázquez, C. Savaniu and S. N. Savvin, *Energy Environ. Sci.*, 2010, **3**, 1670.
46 I. Gibson, D. Rosen and B. Stucker, *Book Additive Manufacturing Technologies*, Springer Science+Business Media LLC, NY, USA, 2010, ch. 11.
47 A. M. Sukeshini, R. Cummins, T. L. Reitz and R. M. Miller, *Electrochem. Solid-State Lett.*, 2009, **12**, B176.
48 G. D. Han, K. C. Neoh, K. Bae, H. J. Choi, S. W. Park, J. W. Son and J. H. Shim, *J. Power Sources*, 2016, **306**, 503.
49 C. Li, H. Chen, H. Shi, M. O. Tadé and Z. Shao, *J. Power Sources*, 2015, **273**, 465.
50 N. Yashiro, T. Usui and K. Kikuta, *J. Eur. Ceram. Soc.*, 2010, **30**, 2093.
51 A. M. Sukeshini, F. Meisenkothen, P. Gardner and T. L. Reitz, *J. Power Sources*, 2014, **224**, 295.
52 A. M. Sukeshini, P. Gardner, F. Meisenkothen, T. Jenkins, R. Miller, M. Rottmayer and T. L. Reitz, *ECS Trans.*, 2011, **35**, 2151.
53 H. Shimada, F. Ohba, X. Li, A. Hagiwara and M. Ihara, *J. Electrochem. Soc.*, 2012, **159**, F360.
54 E. H. Da'as, J. T. S. Irvine, E. Traversa and S. Boulfrad, *ECS Trans.*, 2013, **57**, 1851.
55 M. Dudek, R. I. Tomov, C. Wang, B. A. Glowacki, P. Tomczyk, R. P. Socha and M. Mosialek, *Electrochim. Acta*, 2013, **105**, 412.
56 R. D. Farahani, K. Chizari and D. Therriault, *Nanoscale*, 2014, **6**, 10470.
57 E. M. Hernández-Rodríguez, P. Acosta-Mora, J. Méndez-Ramos, E. Borges Chinea, P. Esparza Ferrera, J. Canales-Vázquez, P. Núñez and J. C. Ruiz-Morales, *Bol. Soc. Esp. Ceram. Vidrio*, 2014, **53**, 213.
58 A. E. Jakus, S. L. Taylor, N. R. Geisendorfer, D. C. Dunand and R. N. Shah, *Adv. Funct. Mater.*, 2015, **25**, 6985.
59 R. Shah, *Fuel Cells Bull.*, 2015, **2015**, 11.
60 Cell3Ditor, www.cell3ditor.eu.
61 K. Sun, T. S. Wei, B. Y. Ahn, J. Y. Seo, S. J. Dillon and J. A. Lewis, *Adv. Mater.*, 2013, **25**, 4539.
62 Y. Hu and X. Sun, *J. Mater. Chem. A*, 2014, **2**, 10712.
63 J. W. Long, B. Dunn, D. R. Rolison and H. S. White, *Chem. Rev.*, 2004, **104**, 4463.
64 J. S. Sakamoto and B. Dunn, *J. Mater. Chem.*, 2002, **12**, 2859.
65 J. Liu, H. G. Zhang, J. Wang, J. Cho, J. H. Pikul, E. S. Epstein, X. Huang, J. Liu, W. P. King and P. V. Braun, *Adv. Mater.*, 2014, **26**, 7096.
66 J. Jiang, Y. Li, J. Liu, X. Huang, C. Yuan and X. W. Lou, *Adv. Mater.*, 2002, **24**, 5166.
67 M. M. Shaijumon, E. Perre, B. Daffos, P.-L. Taberna, J.-M. Tarascon and P. Simon, *Adv. Mater.*, 2010, **22**, 4978.
68 P. H. L. Notten, F. Roozeboom, R. A. H. Niessen and L. Baggetto, *Adv. Mater.*, 2007, **19**, 4564.
69 C. Zhao, C. Wang, R. Gorkin III, S. Beirne, K. Shu and G. G. Wallace, *Electrochem. Commun.*, 2014, **41**, 20.
70 S. Lawes, A. Riese, Q. Sun, N. Cheng and X. Sun, *Carbon*, 2015, **92**, 150.
71 S. R. Gowda, A. L. M. Reddy, X. Zhan and P. M. Ajayan, *Nano Lett.*, 2011, **11**, 3329.
72 N. Li, Z. Chen, W. Ren, F. Li and H.-M. Cheng, *Proc. Natl. Acad. Sci. U. S. A.*, 2012, **109**, 17360.
73 C. Zhu, T. Y.-J. Han, E. B. Duoss, A. M. Golobic, J. D. Kuntz, C. M. Spadaccini and M. A. Worsley, *Nat. Commun.*, 2015, **6**, 6962.
74 J. H. Kim, W. S. Chang, D. Kim, J. R. Yang, J. T. Han, G.-W. Lee, J. T. Kim and S. K. Seol, *Adv. Mater.*, 2015, **27**, 157.
75 R. R. Kohlmeyer, A. J. Blake, J. O. Hardin, E. A. Carmona, J. Carpena-Núñez, B. Maruyama, J. D. Berrigan, H. Huang and M. F. Durstock, *J. Mater. Chem. A*, 2016, **4**, 16856.
76 R. E. Garcia and Y.-M. Chiang, *J. Electrochem. Soc.*, 2007, **154**, A856.
77 S. Ranganathan, R. McCreery, S. M. Majji and M. Madou, *J. Electrochem. Soc.*, 2000, **147**, 277.
78 X. Liu, R. Jervis, R. C. Maher, I. J. Villar-Garcia, M. Naylor-Marlow, P. R. Shearing, M. Ouyang, L. Cohen, N. P. Brandon and B. Wu, *Adv. Mater. Technol.*, 2016, **1**, 1.
79 J. H. Pikul, H. G. Zhang, J. Cho, P. V. Braun and W. P. King, *Nat. Commun.*, 2013, **4**, 1732.
80 Y. Zhu, S. Murali, M. D. Stoller, K. J. Ganesh, W. Cai, P. J. Ferreira, A. Pirkle, R. M. Wallace, K. A. Cychosz, M. Thommes, D. Su, E. A. Stach and R. S. Ruoff, *Science*, 2011, **332**, 1537.
81 C. Liu, Z. Yu, D. Neff, A. Zhamu and B. Z. Jang, *Nano Lett.*, 2010, **10**, 4863.
82 M. D. Stoller and R. S. Ruoff, *Energy Environ. Sci.*, 2010, **3**, 1294.
83 H. Ning, J. H. Pikul, R. Zhang, X. Li, S. Xu, J. Wang, J. A. Rogers, W. P. King and P. V. Braun, *Proc. Natl. Acad. Sci. U. S. A.*, 2015, **112**, 6573.
84 G. Nyström, A. Marais, E. Karabulut, L. Wågberg, Y. Cui and M. M Hamedi, *Nat. Commun.*, 2015, **6**, 7259.
85 G. Sun, J. An, C. K. Chua, H. Pang, J. Zhang and P. Chen, *Electrochem. Commun.*, 2015, **51**, 33.
86 L. T. Le, M. H. Ervin, H. Qiu, B. E. Fuchs and W. Y. Lee, *Electrochem. Commun.*, 2011, **13**, 355.
87 Y. Gu, A. Wu, H. Sohn, C. Nicoletti, Z. Iqbal and J. F. Federici, *J. Manuf. Process.*, 2015, **20**, 198.
88 Y. Zhao, Q. Zhou, L. Liu, J. Xu, M. Yan and Z. Jiang, *Electrochim. Acta*, 2006, **51**, 2639.
89 S. D. Lawes, Inkjet Printed Thin Film Electrodes for Lithium-Ion Batteries, PhD thesis, The University of Western Ontario, 2015.
90 L. T. Le, M. H. Ervin, H. Qiu, B. E. Fuchs, J. Zunino and W. Y. Lee, Inkjet-printed graphene for flexible micro-supercapacitors, presented at the 11th IEEE Intl. Conf. on Nanotech., Portland, Oregon, 2011, p. 67.
91 M. H. Ervin, L. T. Le and W. Y. Lee, *Electrochim. Acta*, 2014, **147**, 610.
92 C. C. Ho, K. Murata, D. A. Steingart, J. W. Evans and P. K. Wright, *J. Micromech. Microeng.*, 2009, **19**, 094013.
93 Y. Yang, S. Jeong, L. Hu, H. Wu, S. W. Lee and Y. Cui, *Proc. Natl. Acad. Sci. U. S. A.*, 2011, **108**, 13013.
94 S.-H. Kim, K.-H. Choi, S.-J. Cho, S. Choi, S. Park and S.-Y. Lee, *Nano Lett.*, 2015, **15**, 5168.

95 K. Sun, Fabrication and Demonstration of High Energy Density Lithium ion microbatteries, PhD thesis, University of Illinois, Urbana-Champaign, 2015.
96 ''Procedure for ceramic slurry to fabricate filaments for 3D printing'', J. Canales-Vázquez, G. B. Sánchez-Bravo, J. R. Marín-Rueda, V. Yagüe-Alcaraz, J. J. López, P201630581 (patent pending), 2016.
97 F. C. Krebs, *Sol. Energy Mater. Sol. Cells*, 2009, **93**, 394.
98 D. Vak, K. Hwang, A. Faulks, Y.-S. Jung, N. Clark, D.-Y. Kim, G. J. Wilson and S. E. Watkins, *Adv. Energy Mater.*, 2015, **5**, 1.
99 K. Hwang, Y.-S. Jung, Y.-J. Heo, F. H. Scholes, S. E. Watkins, J. Subbiah, D. J. Jones, D.-Y. Kim and D. Vak, *Adv. Mater.*, 2015, **27**, 1241.
100 F. Di Giacomo, A. Fakharuddin, R. Jose and T. M. Brown, *Energy Environ. Sci.*, 2016, **9**, 3007.
101 J. Yoon, *et al.*, *Nat. Mater.*, 2008, **7**, 907.
102 Y. T. Gizachew, L. Escoubas, J. J. Simon, M. Pasquinelli, J. Loiret, P. Y. Leguen, J. C. Jimeno, J. Martin, A. Apraiz and J. P. Aguerre, *Sol. Energy Mater. Sol. Cells*, 2011, **95**, 70.
103 Y. Galagan, E. W. C. Coenen, S. Sabik, H. H. Gorter, M. Barink, S. C. Veenstra, J. M. Kroon, R. Andriessen and P. W. M. Blom, *Sol. Energy Mater. Sol. Cells*, 2012, **104**, 32.
104 Y. Jiang, Y. Chen, M. Zhang, Y. Qiu, Y. Lin and F. Pan, *RSC Adv.*, 2016, **6**, 51871.
105 http://www.abc.net.au/radionational/programs/scienceshow/perovskites-show-promise-for-the-next-big-jump-in-solar-cells/6507414, accessed December 2016.
106 B. Y. Ahn, E. B. Duoss, M. J. Motala, X. Guo, S. Park, Y. Xiong, J. Yoon, R. G. Nuzzo, J. A. Rogers and J. A. Lewis, *Science*, 2009, **323**, 1590.
107 B. Y. Ahn, D. J. Lorang, E. B. Duoss and J. A. Lewis, *Chem. Commun.*, 2010, **46**, 7118.
108 B. Myers, M. Bernardi and J. C. Grossman, *Appl. Phys. Lett.*, 2010, **96**, 071902.
109 M. Bernardi, N. Ferralis, J. H. Wan, R. Villalon and J. C. Grossman, *Energy Environ. Sci.*, 2012, **5**, 6880.
110 L. van Dijk, E. A. P. Marcus, A. J. Oostra, R. E. I. Schropp and M. Di Vece, *Sol. Energy Mater. Sol. Cells*, 2015, **139**, 19.
111 L. van Dijk, U. W. Paetzold, G. A. Blab, R. E. I. Schropp and M. Di Vece, *Prog. Photovoltaics*, 2016, **24**, 623.
112 A. Braun, E. A. Katz, D. Feuermann, B. M. Kayes and J. M. Gordon, *Energy Environ. Sci.*, 2013, **6**, 1499.
113 J. de Wild, A. Meijerink, J. K. Rath, W. G. J. H. M. van Sark and R. E. I. Schropp, *Energy Environ. Sci.*, 2011, **4**, 4835.
114 F. Auzel, *Chem. Rev.*, 2004, **104**, 139.
115 G. E. Arnaoutakis, J. Marques-Hueso, A. Ivaturi, K. W. Krämer, S. Fischer, J. C. Goldschmidt and B. S. Richards, *Opt. Express*, 2014, **22**, A452.
116 G. E. Arnaoutakis, J. Marques-Hueso, A. Ivaturi, S. Fischer, J. C. Goldschmidt, K. W. Krämer and B. S. Richards, *Sol. Energy Mater. Sol. Cells*, 2015, **140**, 217.
117 J. W. Choi, H. C. Kim and R. Wicker, *J. Mater. Process. Technol.*, 2011, **211**, 318.
118 www.luxexcel.com.
119 J. S. Price, X. Sheng, B. M. Meulblok, J. A. Rogers and N. C. Giebink, *Nat. Commun.*, 2015, **6**, 6223.
120 J. C Ruiz-Morales, J. Méndez-Ramos, P. Acosta-Mora, M. E. Borges and P. Esparza, *J. Mater. Chem. C*, 2014, **2**, 2944.
121 J. Méndez-Ramos, J. C. Ruiz-Morales, P. Acosta-Mora and N. M. Khaidukovc, *J. Mater. Chem. C*, 2016, **4**, 801.
122 M. G. Debije and P. P. C. Verbunt, *Adv. Energy Mater.*, 2012, **2**, 12.
123 Q. Ge, A. H. Sakhaei, H. Lee, C. K. Dunn, N. X. Fang and M. L. Dunn, *Sci. Rep.*, 2016, **6**, 31110.
124 X. Guo, *et al.*, *Proc. Natl. Acad. Sci. U. S. A.*, 2009, **106**, 20149.
125 Y. de Hazan, M. Thänert, M. Trunec and J. Misak, *J. Eur. Ceram. Soc.*, 2012, **32**, 1187.
126 M. Scheffler and P. Colombo, in *Book Cellular Ceramics: Structure, Manufacturing, Properties and Applications*, ed. M. Scheffler and P. Colombo, Wiley-VCH GmbH, Weinheim, 2005, p. 454.
127 J. Van Noyen, S. Mullens, F. Snijkers and J. Luyten, *WIT Trans. Ecol. Environ.*, 2011, **154**, 93.
128 F. M. Dautzenberg and M. Mukherjee, *Chem. Eng. Sci.*, 2001, **56**, 251.
129 J. A. Moulijn and F. Kapteijn, *Curr. Opin. Chem. Eng.*, 2013, **2**, 346.
130 C. R. Tubío, J. Azuaje, L. Escalante, A. Coelho, F. Guitián, E. Sotelo and A. Gil, *J. Catal.*, 2016, **334**, 110.
131 M. D. Symes, P. J. Kitson, J. Yan, C. J. Richmond, G. J. T. Cooper, R. W. Bowman, T. Vilbrandt and L. Cronin, *Nat. Chem.*, 2012, **4**, 349.
132 M. R. Skorski, J. M. Esenther, Z. Ahmed, A. E. Miller and M. R. Hartings, *Sci. Technol. Adv. Mater.*, 2016, **17**, 89.
133 H. Thakkar, S. Eastman, A. Hajari, A. A. Rownaghi, J. C. Knox and F. Rezaei, *ACS Appl. Mater. Interfaces*, 2016, **8**, 27753.
134 S. Couck, J. Lefevere, S. Mullens, L. Protasova, V. Meynen, G. Desmet, G. V. Baron and J. F. M. Denayer, *Chem. Eng. J.*, 2017, **308**, 719.